


Hard antiphase domain boundaries in strontium titanate: A comparison of Landau-Ginzburg-Devonshire and *ab initio* results

A. Tröster^{1,*}, J. Pils¹, F. Bruckner¹, I. Rychetsky², C. Verdi³ and W. Schranz¹

¹University of Vienna, Faculty of Physics, Boltzmannngasse 5, A-1090 Vienna, Austria

²Institute of Physics, Academy of Sciences of the Czech Republic, Na Slovance 2, 18221 Prague 8, Czech Republic

³School of Mathematics and Physics, The University of Queensland, Brisbane, Queensland 4072, Australia

 (Received 12 June 2023; revised 8 September 2023; accepted 3 October 2023; published 17 October 2023)

Recently, the emergence of polarity of so-called hard antiphase boundaries in strontium titanate was investigated using atomistic simulations based on machine-learned force fields. Comparing the resulting order parameter (OP) and polarization profiles to those obtained from numerical solutions based on a well-established Landau-Ginzburg-Devonshire (LGD) parametrization produces good agreement of the structural OP amplitudes but fails dramatically in reproducing the shape and pressure behavior of the domain wall (DW) polarization. While the atomistic simulations yield a nonzero DW polarization up to at least 120 kbar, LGD theory would predict a sharp transition to zero at a pressure as low as 4.6 kbar. A semiquantitative agreement can be restored by adding so-called rotopolar couplings to the LGD potential and by considering the effects of nuclear quantum fluctuations. Additional evidence for the correctness of our extensions of the LGD approach is provided by comparing the temperature dependence of the DW polarization to recent experimental depolarization pyrocurrent measurements. Our results illustrate the importance of accounting for nuclear quantum effects beyond standard atomistic approaches in the investigation of DW properties.

DOI: [10.1103/PhysRevB.108.144108](https://doi.org/10.1103/PhysRevB.108.144108)

I. INTRODUCTION

The electric and magnetic properties of domain walls (DWs) continue to attract a great deal of attention in contemporary solid-state research. In contrast to the static heterointerfaces between metal-oxides in existing electronic devices, DWs in ferroics constitute highly reactive interfacial structures that may be created, annihilated, recreated, and moved around while exhibiting a number of exciting physical properties that are absent in the bulk phases. The current fundamental research in this field, for which the term *domain wall engineering* has been coined [1], may pave the way for the development of exciting types of ferroelectric devices that could offer enormous flexibility as well as performance. The flurry of recent scientific activity on DWs and other topological defects in polar oxide nanostructures was recently reviewed in Ref. [2], and it is safe to predict that research on the intriguing properties of DWs and other inhomogeneous structures will only intensify in the years to come.

Among the many fascinating topics of this field, the possibility of the emergence of a nonzero polarity in the vicinity of a DW separating nonpolar bulk phases constitutes a particularly interesting subject. A prototypical example to study this scenario is that of DWs in strontium titanate (STO) and other perovskites, a key material class for nanoelectronics. A variety of modern theoretical and computational methods has been applied to analyze such problems. Layer group analysis [3,4] can provide valuable insights into the symmetry

constraints governing the physical phenomena that can emerge in the vicinity of the DW. Based on the phenomenology and symmetry analysis of the thermodynamics of the bulk phases and their fluctuation behavior, Landau-Ginzburg-Devonshire (LGD) theory offers the possibility to predict DW profile shapes numerically [5]. As to atomistic simulations, the case of hard antiphase boundaries (APBs; this terminology is explained in detail in Sec. II) in STO is particularly challenging due to their width, which may span over many lattice constants at low pressures. Hence, structural relaxations based on standard density functional theory (DFT) [6], while confined to zero temperature, are difficult to converge since both large supercells and tight force thresholds are required. To mitigate computational bottlenecks of fully atomistic approaches, sophisticated extensions [7,8] of effective Hamiltonian models [9–12] have been worked out, and such models were also applied to study DWs in STO [13,14].

Recent advancements in applying machine-learning strategies to learn energies and forces in condensed matter systems [15,16] offer an attractive alternative to overcome the limitations of fully atomistic approaches. In Ref. [17], DW profiles for hard APBs in STO were computed from structural relaxations in which forces calculated from DFT were replaced by a machine-learned force field (MLFF). Interestingly, the properties of the resulting structural order parameter (OP) and polarization profiles disagreed with those of earlier *ab initio* results of Ref. [6]. In contrast, however, excellent agreement was found between the structural OP profiles obtained using the MLFF and those resulting from an analytic approximation derived from LGD theory above pressures of 20 kbar. In this analytic approximation, however, polarization effects had

*andreas.troester@univie.ac.at

been neglected. In this paper, we undertake a full numerical analysis of the pressure behavior of the DW profiles of both structural OP and polarization as calculated from LGD theory. We demonstrate that the pressure behavior of the polarization profiles numerically calculated from the well-established LGD parametrization of Ref. [5] is not only completely incompatible with that reported in Ref. [6] but also with what is observed in Ref. [17].

LGD theory and atomistic simulations based on first-principles methods are complementary and often even mutually supportive methods in the science of ferroelectric phenomena. Understanding the underlying reasons for the disagreement of these two indispensable tools and restoring compatibility of both approaches is therefore vital. In this paper, we disentangle the reasons for the inconsistencies listed above and give a correct interpretation of the underlying physics. In doing so, we highlight (i) the effects of quantum fluctuations so far neglected in atomistic simulations of DW properties, and (ii) the importance of including rotopolar couplings (RPCs), providing guidelines for systematic studies of DW properties via both atomistic simulations and phenomenological theories.

II. SURVEY OF HARD APB PROFILES OBTAINED FROM SIMULATIONS AND LGD THEORY

As mentioned in the introduction, the DW profiles obtained from the DFT simulations of Ref. [6], the MLFF-based atomistic simulations of Ref. [17], and the profiles obtained from numerically minimizing the LGD potential discussed in Ref. [5] are in mutual disagreement in several key aspects. Following a short introduction to the basic LGD description of hard APBs, we start with a brief review of these approaches.

At room temperature, STO exhibits the simple cubic perovskite structure with space group $G = Pm\bar{3}m$, but at $T_c = 105$ K, it undergoes an antiferrodistortive structural phase transition to a tetragonal phase of $I4/mcm$ symmetry with a doubling of the unit cell. It had been recognized [18] and verified in countless following papers that this transition is due to static rotations of the TiO_6 octahedra around one of the cubic axes \mathbf{a}_i , $i = 1, 2, 3$ in an alternating pattern with wave vector $\mathbf{k}_R = \frac{2\pi}{a}(\frac{1}{2}\frac{1}{2}\frac{1}{2})$, whose respective rotation angles ϕ_i represent the components of a three-dimensional OP $\Phi = (\phi_1, \phi_2, \phi_3)$ (see Fig. 1 for an illustration) transforming according to the active irreducible representation R_4^+ (for more details see, e.g., Ref. [19]).

With three possible orientations $S = 1, 2, 3$ and two choices of alternating phase $i = 1, 2$, the symmetry reduction at the transition will therefore produce one out of $3 \times 2 = 6$ possible domain states which we label as S_i . Two different domains S_i, S'_i may therefore differ in their OP direction, i.e., their direction of tetragonal axis, and/or their phase. Since the transition is also accompanied by the appearance of spontaneous strain along the respective tetragonal axis, DWs between pairs of domains with unequal orientations $S \neq S'$ and thus conflicting spontaneous strains are generally accompanied by inhomogeneous strain patterns and are therefore called ferroelastic. In this paper, we instead focus on DWs between pairs of domains S_1, S_2 with equal orientation but a jump in the alternating rotation pattern.

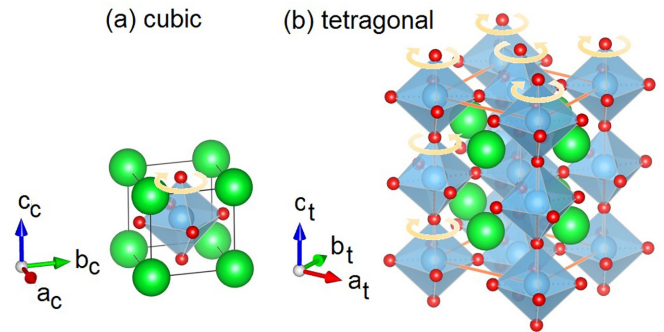


FIG. 1. Illustration of the physical meaning of the three-dimensional structural order parameter (OP) Φ of STO and the doubling of the unit cell passing from (a) cubic $Pm\bar{3}m$ to (b) tetragonal $I4/mcm$ symmetry (shown is the conventional unit cell). $\mathbf{a}_c, \mathbf{b}_c, \mathbf{c}_c$ and $\mathbf{a}_t, \mathbf{b}_t, \mathbf{c}_t$ refer to the directions of the cubic and tetragonal basis vectors, respectively. Drawings done with VESTA [20].

As in our previous work [17], we shall without loss of generality follow the convention $S = 3$, i.e., we shall assume that the equilibrium OPs $(0, 0, \pm\bar{\phi})$ of both domains $3_1, 3_2$ point along the 3 axis of our coordinate system. In principle, this still leaves an infinite number of possible DW configurations, which are further characterized by the unit vector \mathbf{n} normal to the DW and its atomic positioning. However, most of these geometrically possible configurations are energetically extremely unfavorable, and in practice, only very few relevant possibilities remain. Assuming \mathbf{n} to point along the 1 direction and placing the DW central plane at a layer of Sr atoms, the jump in the octahedral rotation pattern across the DW would obviously conflict with the requirement that neighboring oxygen octahedra always must share a common oxygen atom [Fig. 2(b)]. Hence, a kind of geometric frustration effect emerges in this setting, which would lead to severe deformations of the oxygen octahedra. Distorting their covalent bonds would create enormous energy costs. In reality, therefore, the profile of such a hard [5] APB spreads out over many lattice constants since distributing the associated strain energy smoothly over a larger region is much more favorable

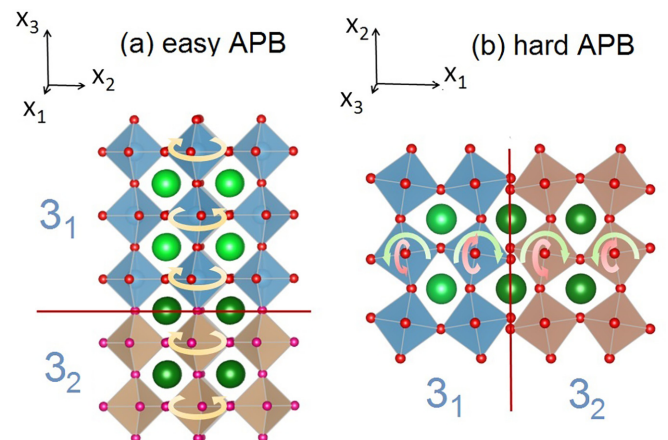


FIG. 2. (a) Sketch of an easy antiphase boundary (APB). (b) Sketch of the geometrical frustration underlying the formation of a hard APB. Drawings done with VESTA [20].

energetically than creating a sharp and abrupt profile with severe covalent distortions. It is precisely the considerable width of such a hard APB that makes it so difficult to tackle its properties with conventional *ab initio* methods. In contrast, if we consider a wall with unit normal \mathbf{n} parallel to the bulk OP direction, such a competition for shared oxygen positions does not arise [cf. Fig. 2(a)], leading to a much thinner easy APB [5], as has been directly verified experimentally using electron diffraction in transmission electron microscopy [21]). To investigate the types of APBs discussed with *ab initio* methods, suitable supercells must be prepared. Therefore, it should be obvious that simulating hard APBs is computationally much more demanding than easy ones. With this in mind, let us briefly review the previous work devoted to this problem.

In Ref. [6], initial guesses for the DW profiles were structurally relaxed in supercells using forces derived from *ab initio* simulations using the PBE exchange-correlation functional [22]. The authors observed not only a tanh-like profile of the resulting main structural OP component $\phi_3(r_1)$, but in the vicinity of the DW, they also detected a much smaller symmetric OP component $\phi_1(r_1)$. In addition, while the polarization component $P_2(r_1)$ remained identically zero, they found a nonzero in-plane polarization component $P_3(r_1)$ that decreased with pressure, vanishing >70 kbar. Hence, they were led to propose the existence of a sharp pressure-driven phase transition inside the DW. However, a number of aspects of these simulations are puzzling. For instance, the width of the DWs seems to be practically independent of pressure, which may hint at severe finite-sized effects due to insufficient supercell sizes. In addition, STO being an incipient ferroelectric (see below), it is well known that its tetragonal phase should exhibit ferroelectric instability in conventional DFT simulations with a PBE functional [23]. The apparent absence of any related anomalies in the simulations of Ref. [6] may only be explained by a combination of insufficient supercell size and a too-large force tolerance factor chosen for the structural force relaxations.

Such a polar instability was indeed encountered in the simulations of Ref. [17], which were based on a MLFF trained on data produced from DFT simulations with the PBEsol functional [24]. A stable nonpolar tetragonal bulk phase in STO at $T = 0$ could only be observed by applying a hydrostatic background pressure p in excess of some 10 kbar, as was also verified by tracing out the energy double well of the unstable polar mode at low pressures. Apart from this, a number of interesting features of the local DW polarization profiles were observed, as illustrated in Fig. 3. In fact, $P_2(r_1)$ still remained identically zero, but both a nonzero in-plane polarization $P_3(r_1)$ and a much smaller but well-defined out-of-plane component $P_1(r_1)$ were detected. While decreasing in amplitude, the polarization component $P_3(r_1)$ persists up to the highest imposed pressure of 120 kbar with no tendency to decay to zero (see Fig. 4). In addition, it was also observed that the in-plane polarization can be switched upon reversing the sign of the out-of-plane OP component. Furthermore, in the DW profiles $P_3(r_1)$ shown in Ref. [17], one notices well-defined oscillations (wiggles) at the onsets of the DW region, whose amplitudes decrease but seem to level off at a constant nonzero value with increasing pressure. Their origin and proper interpretation remained unclear. Finally, a

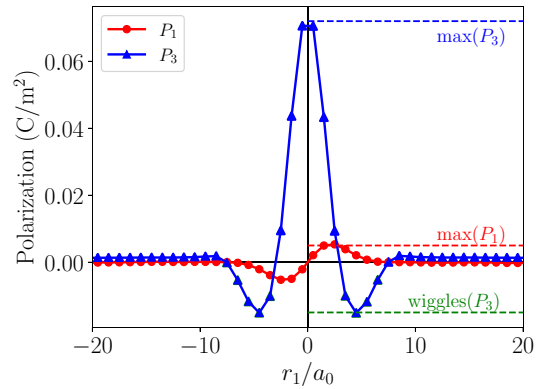


FIG. 3. Illustration of the typical polarization profile features observed in the $T = 0$ K atomistic simulations of Ref. [17] (example taken $p = 60$ kbar).

somewhat smaller but definitely nonzero polarization component $P_1(r_1) = -P_1(-r_1)$ that is odd with respect to spatial reflection about the center of the DW was detected. This is puzzling, since numerically we found that such a longitudinal polarization component, which resembles a localized charge distribution in the vicinity of the DW, should be suppressed by the accompanying dipole-dipole free-energy penalty given by Eq. (S59) in the Supplemental Material (SM) [25].

Somewhat surprisingly, the pressure dependence of the polarization profiles of a hard APB in STO computed from numerically minimizing the LGD Gibbs free energy of Ref. [5] is at odds with either one of these simulation results. Indeed, a straightforward numerical minimization of the LGD free energy functional at $T = 0$ K, according to the prescription of Sec. II in the SM [25], results in a steep decay of the DW polarization. The polarization already vanishes at a critical pressure as low as 4.6 kbar (see Fig. 5), and below this pressure, neither a P_1 component nor any wiggly features of the P_3 profiles are visible. On the other hand, a stable tetragonal bulk phase at 0 K is produced. The above observations clearly indicate that the LGD parametrization of Ref. [5] is partially in contrast with *ab initio*-based simulations. In what follows, we discuss the steps necessary to reconcile atomistic simulations and phenomenological theory.

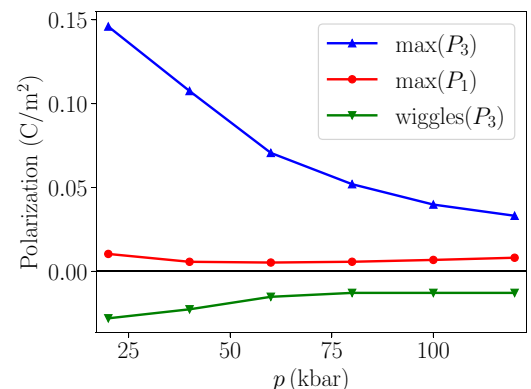


FIG. 4. Pressure dependence of polarization profile features observed in the $T = 0$ K atomistic simulations of Ref. [17].

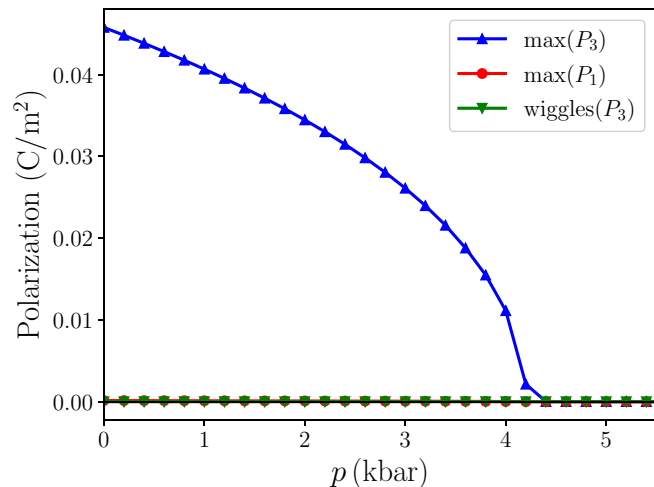


FIG. 5. Pressure dependence of $T = 0$ K polarization amplitudes as computed from Landau-Ginzburg-Devonshire (LGD) theory, calculated using a partial Legendre transform and Tagantsev's parametrization (i.e., without rotopolar couplings).

III. THE ROLE OF NUCLEAR QUANTUM FLUCTUATIONS

The experimental observation that the tetragonal phase of pure STO remains paraelectric down to 0 K dates back to a long time ago. Historically, a pronounced softening of a transverse polar phonon mode and a steep increase of the dielectric constant upon lowering the temperature had been observed [26,27], suggesting a ferroelectric transition at a small but nonzero temperature. However, in the seminal work of Müller and Burkard [28], it was found that the dielectric constant starts to level off ~ 35 K, reaching a finite positive limiting value at 0 K. It was conjectured that only the presence of nuclear quantum fluctuations in STO prevents a transition to a ferroelectric ground state. Nowadays, it is well established that STO is a member of a class of materials known as incipient ferroelectrics, potassium tantalate (KTaO₃), calcium titanate (CaTiO₃), and rutile TiO₂ being other prominent examples [29,30]. Indeed, STO can be driven to the ferroelectric phase by imposing a variety of small external disturbances like isotope substitution [31], electric fields [32], uniaxial [33,34], and epitaxial [35] strain. In the present context, strain-triggered ferroelectricity is of particular relevance given the fact that DWs always induce local inhomogeneous strain fields. Fully consistent with this reasoning, authors of Refs. [36–38] demonstrated that a straightforward calculation of tetragonal STO based on conventional DFT would predict ferroelectric instability at $T = 0$, and the correct physics may only be restored by including the effects of nuclear quantum fluctuations via a subsequent quantum path-integral Monte Carlo simulation. This instability within DFT was corroborated in numerous subsequent works employing more sophisticated exchange-correlation functionals (see, e.g., Ref. [23]).

Within phenomenological LGD theory, the impact of nuclear quantum fluctuation effects on a LGD parametrization has been studied extensively in, e.g., Refs. [39–43]. It was found that they manifest themselves through a pronounced nonlinear temperature behavior of the quadratic coefficients

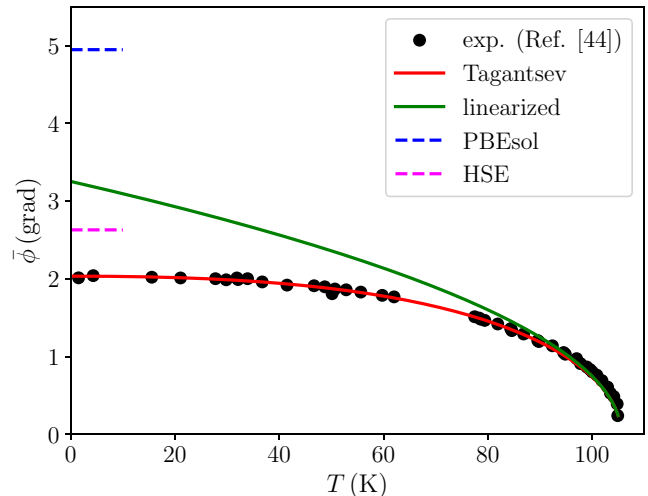


FIG. 6. Comparison of different estimates for the octahedral tilt angle $\bar{\phi}$ at zero pressure. Experimental data (black dots) from Hayward *et al.* [44] fitted by the parametrization of Ref. [5] (red), prediction from linearization (green), and calculations using DFT/PBEsol (blue) and DFT/HSE [23] (magenta).

$a_1(T)$, $b_1(T)$ governed by the so-called Barrett formula [40], while all other coupling coefficients may still remain T -independent, in line with traditional Landau theory [44]. The LGD potential parametrized in Ref. [5] was obtained from fitting experimental data to a LGD theory of this type and indeed concisely reproduces the low-temperature behavior of the structural OP, as seen in Fig. 6. On the other hand, the atomistic simulations of Ref. [17] lack the effects of nuclear quantum fluctuations. In principle, these can be included by using path-integral quantum simulation methods [45] or the stochastic self-consistent harmonic approximation, as recently demonstrated for quantum paraelectric materials [46,47]. Given the complexities resulting from the large supercell sizes and the inhomogeneity, here, we resort to a different strategy to reconcile the pressure dependence of the profiles observed in our previous MLFF calculations with numerical results obtained using LGD theory. Specifically, we reverse-engineer the above Barrett-like temperature dependence of the phenomenological parametrization of Ref. [5]. To do so, we linearize the T dependence of the quadratic coefficients $a_1(T)$, $b_1(T)$ by simple Taylor expansions around the cubic-to-tetragonal transition temperature $T_c = 105$ K, as shown in panels (a) and (b) of Fig. 7. This should result in effectively switching off the effects of quantum fluctuations in the LGD description. While such a shirt-sleeved replacement may seem rather drastic, its validity can be checked by, e.g., comparing the resulting predictions of several bulk observables from LGD to those obtained from DFT. As panels (a) and (b) of Fig. 7 illustrate, a prominent consequence of the linearization is that the zero temperature values $a_1(0)$, $b_1(0)$ obtained for the linearized versions of the LGD coefficients $a_1(T)$, $b_1(T)$ are much lower than the original ones. Since these two coefficients directly control the phase stability in LGD theory, this has profound consequences in the low-temperature regime. For example, we study the zero-temperature limit of the modulus of the structural OP

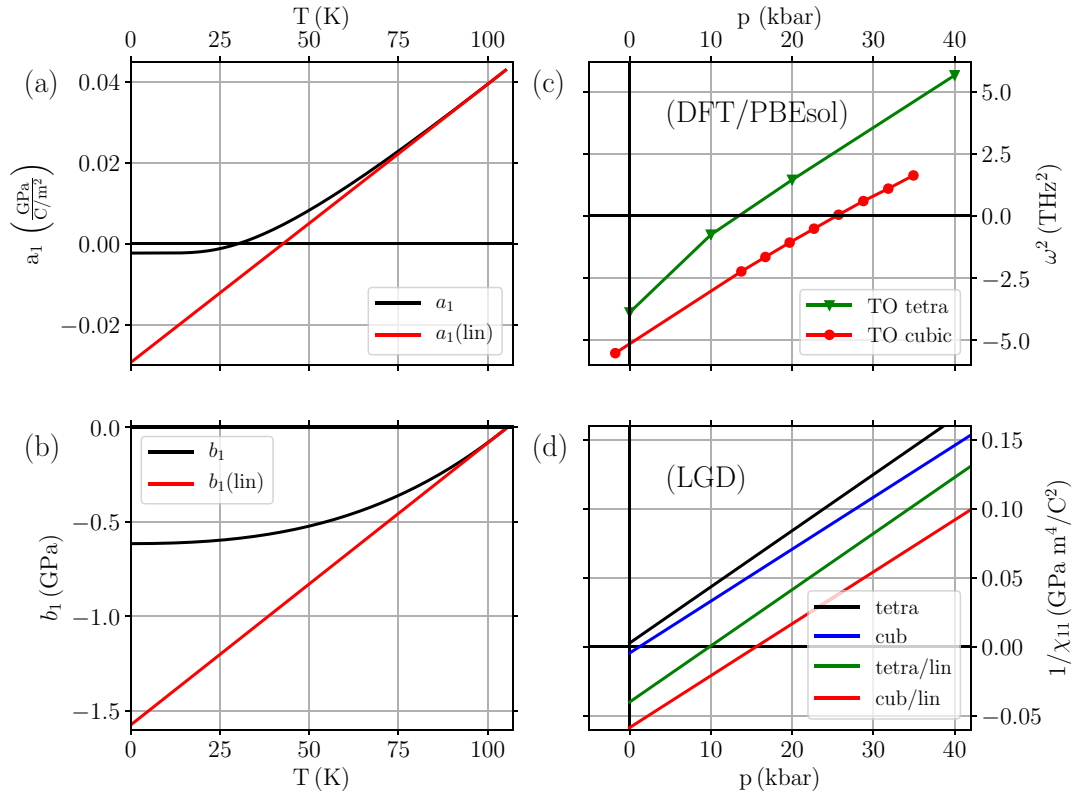


FIG. 7. (a) Original and linearized temperature dependence of Landau-Ginzburg-Devonshire (LGD) parameter function $a_1(T)$. (b) Same for LGD parameter function $b_1(T)$. (c) Pressure dependence of lowest transverse polar phonon mode in the cubic and tetragonal phase of STO at $T = 0$ as computed from density functional theory (DFT) with the PBEsol exchange-correlation functional. (d) Pressure dependence of the inverse susceptibility component χ_{11}^{-1} in the tetragonal and cubic phases of STO at $T = 0$ (continued into unstable regions) as calculated from LGD theory using the original parametrization of Ref. [5] (black and blue curves) and the present linearization of the functions $a_1(T)$, $b_1(T)$ (green and red curves).

represented by the tilt angle $\bar{\phi}$ of the TiO_6 octahedra in the tetragonal phase. Figure 6 shows a comparison of different values for $\bar{\phi}$ obtained from DFT, experiment, and LGD theory, the latter with and without the above linearization. As expected, the linearization results in a much larger value of $\bar{\phi}$ than the experimental one and is closer to the results obtained from DFT. On the other hand, since the values of $\bar{\phi}$ obtained using various exchange-correlation functionals differ, it is difficult to assess this comparison on a more quantitative level.

Further evidence for the at least semiquantitative validity of our approach to switch off quantum fluctuations in LGD theory is provided by a comparison of the pressure dependence of the squared transverse optical phonon frequencies in the cubic and tetragonal phases calculated from DFT at zero temperature with that of the inverse dielectric susceptibility components χ_{11}^{-1} calculated from LGD theory in both parametrizations. These quantities are shown in panels (c) and (d) of Fig. 7, respectively. Upon linearization, the agreement between DFT and LGD theory improves significantly. In the tetragonal phase, the transverse optical (TO) phonon becomes unstable around $p = 13$ kbar. Based on Tagantsev's LGD parametrization, χ_{11}^{-1} remains stable down to $p = 0$ in the tetragonal phase due to the nuclear quantum fluctuations, whereas in our linearized version, the

instability sets in at $p = 10$ kbar, in much better agreement with DFT.

If we calculate pressure-dependent polarization profiles at $T = 0$ using the linearizations of $a_1(T)$ and $b_1(T)$ discussed above, we obtain the results shown in Fig. 8. In comparison with Fig. 5, the pressure at which $P_3(r_1 = 0)$ vanishes has

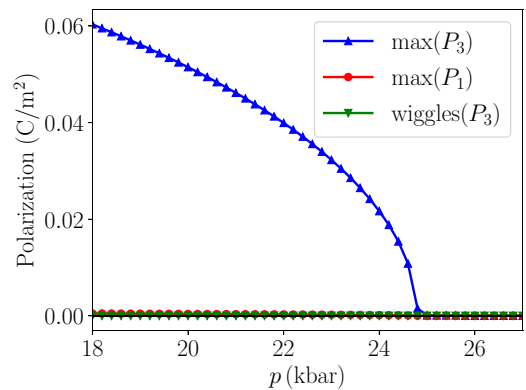


FIG. 8. Pressure dependence of polarization amplitudes at $T = 0$ as calculated from a partially Legendre-transformed Landau-Ginzburg-Devonshire (LGD) free energy in the parametrization of Tagantsev *et al.* [5] but with linearized temperature terms.

been shifted from 4.6 kbar to ~ 25 kbar, so this represents a step in the right direction. To explain the emergence of the large pressure tails of the polarization seen in Fig. 4, the appearance of the nonzero longitudinal polarization component $P_1(r_1)$ and the wiggly features of $P_3(r_1)$ seen in the simulations of Ref. [17] (cf. Fig. 3), we still need to introduce additional so-called RPCs to the free energy.

IV. RPCS

A key observation of Ref. [17] was that the in-plane polarization component profile $P_3(r_1)$ can be switched upon reversing the sign of the out-of plane OP component $\phi_1(r_1)$, which provided compelling evidence to extend the LGD free energy of Ref. [5] by including RPCs. In three dimensions, the general structure of RPC density terms has been discussed before [4,19], where it was shown that they contain precisely four independent coupling constants W_1, \dots, W_4 . In the present quasi-one-dimensional setting, the corresponding coupling density reduces to

$$\begin{aligned} \mathcal{F}_R = & W_1 \left(P_2 \frac{\partial \phi_2}{\partial r_1} + P_3 \frac{\partial \phi_3}{\partial r_1} \right) \phi_1 \\ & + W_2 (P_2 \phi_2 + P_3 \phi_3) \frac{\partial \phi_1}{\partial r_1} \\ & + \frac{P_1}{2} \left[W_3 \frac{\partial (\phi_2^2 + \phi_3^2)}{\partial r_1} + W_4 \frac{\partial (\phi_1^2)}{\partial r_1} \right]. \end{aligned} \quad (1)$$

Unless the W_i 's are all zero, adding RPCs obviously induces the observed symmetry breaking. It was also conjectured that RPCs may be regarded as a kind of external field coupled to $P_3(r_1)$ only locally inside the DW, which only weakly depends on pressure and acts to induce the large pressure tails in P_3 . In fact, the existence and importance of RPCs for understanding the properties of ferroelastic DWs in STO had been suggested before [4,14,19].

In any phenomenological Landau-type approach, the numerical values of the coupling constants W_i are *a priori* unknown and must be determined to match the observed properties. Choosing the values $W/\text{GPa} = (0.25, 0.30, 0.60, -0.80)$ yields the pressure dependencies shown in Fig. 9 derived from the purely local mixed elastic free energy potential (Eq. (S78) in the SM [25]). These profiles display a number of interesting features that underline the presence of RPCs. Indeed, near the DW, both the side wiggles to $P_3(r_1)$ and a nonzero asymmetric amplitude $P_1(r_1)$ that were detected in the atomistic simulations of Ref. [17], and whose origin had not been understood, are now convincingly reproduced. The pressure dependence of their amplitudes is also qualitatively like that found in the simulation data. Moreover, considering the fraction $|\phi_1(0)/\phi_3(0)|$ of structural OP amplitudes ϕ_1 and ϕ_3 at the center of the DW, we obtain the value $|\phi_1(0)/\phi_3(0)| \approx 0.92$ using the present parametrization. This value remains roughly constant for the whole pressure range from 0 to 120 kbar. Remarkably, an identical value is observed in the simulations of Ref. [17], while the corresponding ratio calculated from the OP profile of Ref. [6] is much smaller. In contrast to the pressure-independent DW widths reported in Ref. [6], our LGD parametrization also yields DW widths monotonously

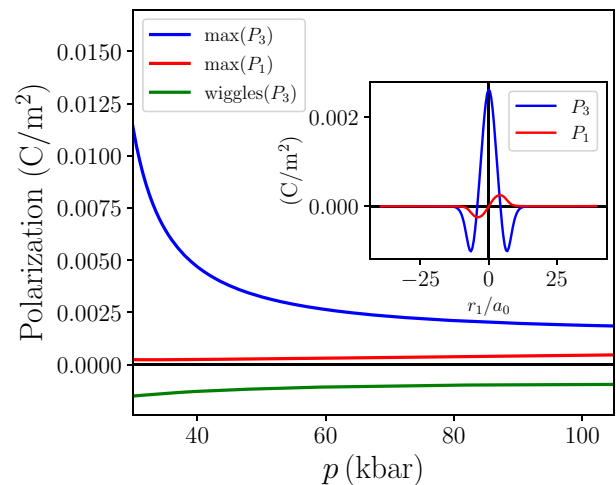


FIG. 9. Main panel: Pressure dependence of polarization amplitudes at $T = 0$ as computed from Landau-Ginzburg-Devonshire (LGD) theory: partial Legendre transform, linearized temperature term, rotopolar couplings $W = (0.25, 0.30, 0.60, -0.80)$. Inset: Sample polarization profiles $P_1(r_1), P_3(r_1)$ at pressure $p = 50$ kbar and $T = 0$.

decreasing from ~ 15 pseudocubic lattice constants a_0 at $p = 30$ kbar to roughly $8a_0$, like what is observed in the atomistic simulations of Ref. [17].

V. EXPERIMENTAL EVIDENCE

Up to this point, we have analyzed the atomistic simulations in which nuclear quantum effects were absent, monitoring their behavior as a function of pressure at zero temperature. To compare the temperature behavior of the polarization profile resulting from our LGD parametrization with any real-world experimental data, we may now simply switch on nuclear quantum fluctuations again by restoring the original Barrett-type nonlinear temperature dependencies of the quadratic LGD coupling terms $a_1(T)$ and $b_1(T)$. Unfortunately, however, up to now, firm experimental data on the ferroelectricity of hard APBs are rare in the published literature. Nevertheless, we believe that there is some, albeit indirect, experimental evidence for a possible temperature effect of hard APBs of ferroelectric origin. In Ref. [48], depolarization pyrocurrent measurements were carried out on polycrystalline samples of STO at low temperatures. Around $T \approx 45$ K, a clear peak of ferroelectric origin in the measured pyrocurrent is observed. Interestingly, using the LGD parametrization obtained above, the temperature derivative of the polarization component $P_3(r_3 = 0)$, which should be proportional to the pyrocurrent, exhibits an extremum ~ 41.2 K (see Fig. 10). Hence, the presence of a DW polarization of the described type may offer an excellent explanation of the otherwise unknown origin of this ferroelectric temperature anomaly in polycrystalline STO.

VI. DISCUSSION AND OUTLOOK

The interplay between experiment, phenomenological theories, and first-principles atomistic simulations is the driving

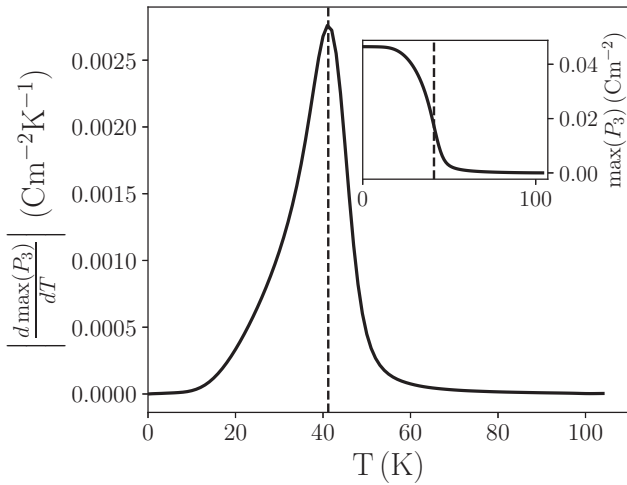


FIG. 10. Main panel: T -dependence of the modulus of the temperature derivative $dP_3(r_1=0)(T)/dT$ of the polarization amplitude $P_3(r_1=0)(T)$ as calculated from LGD theory with the partial Legendre transformation model, restored nonlinear temperature parametrization and rotopolar couplings $W = (0.25, 0.30, 0.60, -0.80)$. Inset: plot of $P_3(r_1=0)(T)$. The temperature $T = 41.2$ K of the extremum of the temperature derivative is indicated by a dashed vertical line.

force for gaining insight into the physics of phase transitions in condensed matter. The concise incorporation of symmetry is the strength of phenomenological approaches like Landau theory, which resembles an expansion in terms of symmetry-allowed invariants. Its Achilles heel lies, however, in the fact that the numerical values of the corresponding expansion coefficients are unknown from the outset and must be determined from fitting its predictions to results obtained from experiment or simulation. Moreover, the expansion must necessarily be truncated at some finite order, and if one thereby fails to include physically relevant couplings, then it may yield even qualitatively wrong predictions. In both of these aspects, our present results demonstrate that STO represents a particularly delicate system. In fact, certain features like the OP amplitude ratio $\phi_1(0)/\bar{\phi} \approx 0.92$ obtained in first-principles simulations were already concisely reproduced by minimizing the unmodified LGD free energy of Ref. [5]. However, to reproduce the properties of the polarization profiles observed in simulations, it is crucial to consider finite-sized effects and to include additional couplings beyond those listed in Ref. [5]. Indeed, for the incipient ferroelectric STO, when the effects of nuclear quantum fluctuations inherently included in the original LGD parametrization are turned off, semiquantitative agreement of the LGD calculation of DW profiles of a hard APB in STO with the results of first-principles simulations is obtained. With these modifications in place, all described qualitative features of the polarization profiles $P_i(r_1)$ are observed to emerge automatically. The inclusion of RPCs simultaneously produces (i) the formation of the peculiar side wiggles in $P_3(r_1)$, (ii) the equally striking appearance of a nonzero asymmetric component $P_1(r_1)$, which in the absence of RPCs would be completely suppressed by the counteracting dipolar interaction [Eq. (S59) in the SM [25]] but had been clearly seen in the atomistic simulations of

Ref. [17], (iii) the large pressure tails in these amplitudes, and (iv) a reasonable pressure dependence of the observed DW widths, which are all in striking qualitative agreement with the ones extracted from the atomistic MLFF simulations.

The most severe numerical discrepancy that prevents our LGD analysis from being fully quantitative is the apparent underestimation of the polarization amplitudes in the linearized LGD theory in comparison with those calculated from the atomistic theory. Moreover, the polarization obtained in Ref. [48], which was estimated to be in excess of 10^{-2} C/m², was obtained by integrating pyrocurrents measured in polycrystalline STO pellets. Due to the implicit directional and inhomogeneity averaging effects, we would therefore expect the measured amplitude to be much smaller than the ideal value calculated from LGD theory. Instead, it appears to be of the same order of magnitude as the polarizations we obtain from our model calculations (see the inset of Fig. 10).

While we can only speculate about the reasons for this quantitative failure, there are several possible shortcomings that may contribute to the observed discrepancies. First, our search for optimal values of RPC parameters W_i was certainly not exhaustive. Numerical tests indicate, however, that their influence on the polarization amplitudes is rather modest for reasonable choices of their values, and thus, we do not believe that the uncertainties in determining the couplings W_i are the main source of the observed polarization magnitude discrepancies. In this context, we should also remind the reader of the plain fact that polarization in STO—being absent in the bulk—is already a second-order effect, and hence, the corresponding numerical values for all polarization-related LGD coupling coefficients are rather difficult to assess from experiment. Therefore, one must be prepared to also consider the possibility that these values may need some revision.

In the closely related case of a ferroelastic DW in STO, the authors of Ref. [14] emphasized that, in addition to the structural OP field Φ , the polarization \mathbf{P} , and the elastic degrees of freedom, it should be essential to consider couplings to a local displacement field U^{Ti} . According to their description, these displacements act exclusively on the titanium atoms in an alternating fashion. They resemble the amplitude of an R -point phonon which, even though not soft, assists in lowering the energy cost of TiO₆ octahedral rotations. As we show in the SM [25], we have indeed been able to identify a corresponding local nonzero amplitude in the atomistic displacement pattern constituting the hard APB in our relaxed supercells. However, in view of the smallness of this amplitude, we conclude that this displacement mode seems to play no appreciable role in shaping hard APB profiles in STO.

In addition, despite being qualitatively correct, our proposed temperature linearization procedure used to switch off the effects of nuclear quantum fluctuations in LGD theory is rather crude. The fact that our linearized LGD model can only reproduce the DFT results obtained with the PBEsol functional on a semiquantitative level at best is also illustrated by a comparison between Figs. 7(c) and 7(d).

These discrepancies are also illustrated by the systematic underestimation of inhomogeneous strains $\eta_\alpha(r_1)$ by our linearized LGD parametrization, as shown in Fig. 11. In Ref. [17], local polarizations were approximately obtained

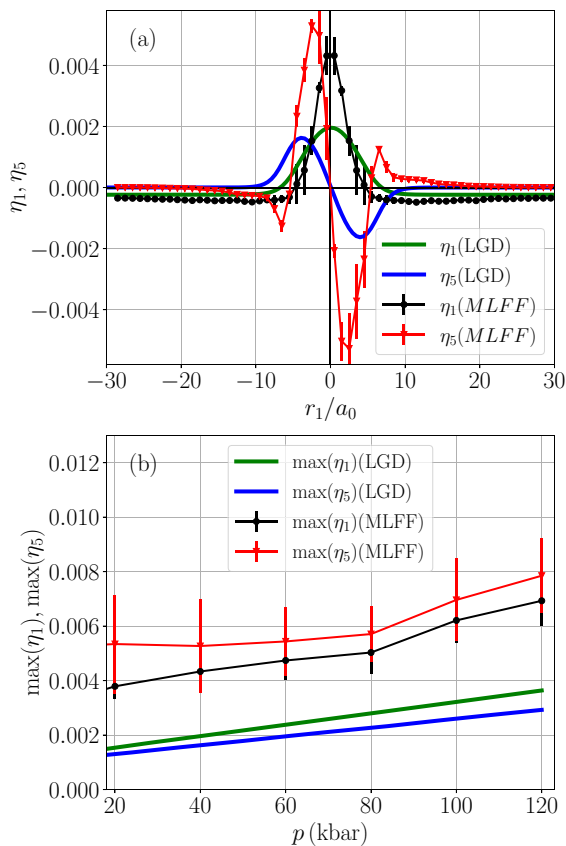


FIG. 11. (a) Comparison of inhomogeneous strain profiles $\eta_1(r_1)$ and $\eta_5(r_1)$ as obtained from the $T = 0$ K machine-learned force field (MLFF) simulations of Ref. [17] at pressure $p = 40$ kbar to those predicted from Landau-Ginzburg-Devonshire (LGD) theory with rot-polar couplings (RPCs) $W = (0.25, 0.30, 0.60, -0.80)$, linearized temperature dependence and mixed Legendre transform at the same pressure and $T = 0$. The negative vertical offsets of both η_1 (LGD) and η_1 (MLFF) are not due to numerical inaccuracy but represent an inevitable finite-sized effect as discussed in Sec. B.2 of the SM [25]. (b) Pressure dependencies of the amplitudes of these inhomogeneous strains at $T = 0$. Error bars in the MLFF data represent the square root of the variances of strain data across the 2×2 cross-sections of the supercells.

following the recipe of Ref. [49], i.e., by multiplying local displacements calculated with respect to a nonpolar reference structure by the corresponding Born effective charge (BEC) tensor calculated for this reference structure. Therefore, underestimating such displacements would linearly affect the resulting polarization amplitudes. Moreover, such a prescription is only numerically meaningful if one accepts the assumption that the BECs are themselves independent of a

deformation path used to relate the final polar to the nonpolar reference structure. There are, however, prominent examples of perovskites for which a pronounced structural dependence of the BECs has been observed (see, e.g., Refs. [50,51]).

We should also not lose sight of the well-known fact [23] that different choices of exchange-correlation functionals generally result in slightly different sets of structural parameters for the bulk unit cells of STO, which can be translated into effective background pressures by which our atomistic results may be shifted. While all of our present simulation results were obtained using the PBEsol exchange-correlation functional, switching to a different exchange-correlation functional may also therefore severely impact the calculated OP and polarization amplitude values, as we had illustrated in Fig. 6, and even the calculated BEC tensor components. It has only recently been recognized how delicate it is to reproduce the anharmonic vibrational effects of STO in an *ab initio* calculation with satisfactory precision [47].

In summary, in this paper, we show that nuclear quantum fluctuations can have a dramatic effect on the low-temperature pressure-dependent DW polarization. These effects must be considered to achieve a quantitative description of DW properties. In a typical LGD framework, in which coefficients are obtained by fitting of experimental data down to low temperatures, such quantum nuclear effects are considered by assuming a Barrett-type temperature dependence of the quadratic potential coefficients. In first-principles-based atomistic studies of DWs, they have been ignored so far. However, such simulations are routinely used to predict the shape and stability of DW profiles or to determine numerical values of LGD coupling parameters. Our findings demonstrate that, to allow a meaningful comparison, one of the two approaches must therefore be modified. In this paper, we switched off nuclear fluctuation effects in the LGD potential by linearizing the corresponding temperature-dependent terms. On the other hand, although this will certainly require a considerable effort, effects of nuclear quantum fluctuations can in principle be accounted for, e.g., with path integral molecular dynamics simulations [37,45] thermostatted with colored noise [52] or the stochastic self-consistent harmonic approximation [47,53,54]. Work in this direction is currently underway in our laboratories.

ACKNOWLEDGMENTS

A.T. acknowledges support by the Austrian Science Fund (FWF) Project No. P27738-N28, and C.V. by FWF Project No. F81-N (SFB TACO) and Australian Research Council Project No. DE220101147. The computational results presented have been achieved in part using the Vienna Scientific Cluster (VSC).

- [1] G. Nataf, M. Guennou, J. Gregg, D. Meier, J. Hlinka, E. Salje, and J. Kreisel, Domain-wall engineering and topological defects in ferroelectric and ferroelastic materials, *Nat. Rev. Phys.* **2**, 634 (2020).
- [2] J. Junquera, Y. Nahas, S. Prokhorenko, L. Bellaiche, J. Íñiguez, D. G. Schlom, L.-Q. Chen, S. Salahuddin, D. A. Muller, L. W.

Martin *et al.*, Topological phases in polar oxide nanostructures, *Rev. Mod. Phys.* **95**, 025001 (2023).

- [3] W. Schranz, I. Rychetsky, and J. Hlinka, Polarity of domain boundaries in nonpolar materials derived from order parameter and layer group symmetry, *Phys. Rev. B* **100**, 184105 (2019).

- [4] W. Schranz, C. Schuster, A. Tröster, and I. Rychetsky, Polarization of domain boundaries in SrTiO₃ studied by layer group and order-parameter symmetry, *Phys. Rev. B* **102**, 184101 (2020).
- [5] A. K. Tagantsev, E. Courtens, and L. Arzel, Prediction of a low-temperature ferroelectric instability in antiphase domain boundaries of strontium titanate, *Phys. Rev. B* **64**, 224107 (2001).
- [6] A. Kvasov, A. K. Tagantsev, and N. Setter, Structure and pressure-induced ferroelectric phase transition in antiphase domain boundaries of strontium titanate from first principles, *Phys. Rev. B* **94**, 054102 (2016).
- [7] P. Ghosez and J. Junquera, Modeling of ferroelectric oxide perovskites: From first to second principles, *Annu. Rev. Condens. Matter Phys.* **13**, 325 (2022).
- [8] J. C. Wojdel, P. Hermet, M. P. Ljungberg, P. Ghosez, and J. Íñiguez, First-principles model potentials for lattice-dynamical studies: general methodology and example of application to ferroic perovskite oxides, *J. Phys.: Condens. Matter* **25**, 305401 (2013).
- [9] W. Zhong, D. Vanderbilt, and K. M. Rabe, Phase transitions in BaTiO₃ from first principles, *Phys. Rev. Lett.* **73**, 1861 (1994).
- [10] W. Zhong, D. Vanderbilt, and K. M. Rabe, First-principles theory of ferroelectric phase transitions for perovskites: The case of BaTiO₃, *Phys. Rev. B* **52**, 6301 (1995).
- [11] K. M. Rabe and U. V. Waghmare, Localized basis for effective lattice Hamiltonians: Lattice Wannier functions, *Phys. Rev. B* **52**, 13236 (1995).
- [12] J. Padilla, W. Zhong, and D. Vanderbilt, First-principles investigation of 180° domain walls in BaTiO₃, *Phys. Rev. B* **53**, R5969 (1996).
- [13] J. C. Wojdel and J. Íñiguez, Ferroelectric transitions at ferroelectric domain walls found from first principles, *Phys. Rev. Lett.* **112**, 247603 (2014).
- [14] A. Schiaffino and M. Stengel, Macroscopic polarization from antiferrodistortive cycloids in ferroelastic SrTiO₃, *Phys. Rev. Lett.* **119**, 137601 (2017).
- [15] E. Bedolla, L. C. Padierna, and R. Castaneda-Priego, Machine learning for condensed matter physics, *J. Phys.: Condens. Matter* **33**, 053001 (2021).
- [16] J. Schmidt, M. R. Marques, S. Botti, and M. A. Marques, Recent advances and applications of machine learning in solid-state materials science, *npj Comput. Mater.* **5**, 83 (2019).
- [17] A. Tröster, C. Verdi, C. Dellago, I. Rychetsky, G. Kresse, and W. Schranz, Hard antiphase domain boundaries in strontium titanate unravelled using machine-learned force fields, *Phys. Rev. Mater.* **6**, 094408 (2022).
- [18] H. Unoki and T. Sakudo, Electron spin resonance of Fe³⁺ in SrTiO₃ with special reference to the 110°K phase transition, *J. Phys. Soc. Jpn.* **23**, 546 (1967).
- [19] W. Schranz, A. Tröster, and I. Rychetsky, Contributions to polarization and polarization switching in antiphase boundaries of SrTiO₃ and PbZrO₃, *J. Appl. Phys.* **128**, 194101 (2020).
- [20] K. Momma and F. Izumi, VESTA 3 for three-dimensional visualization of crystal, volumetric and morphology data, *J. Appl. Crystallogr.* **44**, 1272 (2011).
- [21] S. M. Shapiro, J. D. Axe, G. Shirane, and T. Riste, Critical neutron scattering in SrTiO₃ and KMnF₃, *Phys. Rev. B* **6**, 4332 (1972).
- [22] J. P. Perdew, K. Burke, and M. Ernzerhof, Generalized gradient approximation made simple, *Phys. Rev. Lett.* **77**, 3865 (1996).
- [23] R. Wahl, D. Vogtenhuber, and G. Kresse, SrTiO₃ and BaTiO₃ revisited using the projector augmented wave method: Performance of hybrid and semilocal functionals, *Phys. Rev. B* **78**, 104116 (2008).
- [24] J. P. Perdew, A. Ruzsinszky, G. I. Csonka, O. A. Vydrov, G. E. Scuseria, L. A. Constantin, X. Zhou, and K. Burke, Restoring the density-gradient expansion for exchange in solids and surfaces, *Phys. Rev. Lett.* **100**, 136406 (2008).
- [25] See Supplemental Material at <http://link.aps.org/supplemental/10.1103/PhysRevB.108.144108> for further details of our analytical and numerical approach to derive domain wall profiles from LGD theory, which includes the additional Refs. [55–65].
- [26] R. A. Cowley, Temperature dependence of a transverse optic mode in strontium titanate, *Phys. Rev. Lett.* **9**, 159 (1962).
- [27] R. A. Cowley, Lattice dynamics and phase transitions of strontium titanate, *Phys. Rev.* **134**, A981 (1964).
- [28] K. A. Müller and H. Burkard, SrTiO₃: An intrinsic quantum paraelectric below 4 K, *Phys. Rev. B* **19**, 3593 (1979).
- [29] O. Kvyatkovskii, Quantum effects in incipient and low-temperature ferroelectrics (a review), *Phys. Solid State* **43**, 1401 (2001).
- [30] C. Lee, P. Ghosez, and X. Gonze, Lattice dynamics and dielectric properties of incipient ferroelectric TiO₂ rutile, *Phys. Rev. B* **50**, 13379 (1994).
- [31] M. Itoh, R. Wang, Y. Inaguma, T. Yamaguchi, Y.-J. Shan, and T. Nakamura, Ferroelectricity induced by oxygen isotope exchange in strontium titanate perovskite, *Phys. Rev. Lett.* **82**, 3540 (1999).
- [32] J. Hemberger, P. Lunkenheimer, R. Viana, R. Böhmer, and A. Loidl, Electric-field-dependent dielectric constant and non-linear susceptibility in SrTiO₃, *Phys. Rev. B* **52**, 13159 (1995).
- [33] H. Uwe and T. Sakudo, Stress-induced ferroelectricity and soft phonon modes in SrTiO₃, *Phys. Rev. B* **13**, 271 (1976).
- [34] W. Burke and R. Pressley, Stress induced ferroelectricity in SrTiO₃, *Solid State Commun.* **9**, 191 (1971).
- [35] J. Haeni, P. Irvin, W. Chang, R. Uecker, P. Reiche, Y. Li, S. Choudhury, W. Tian, M. Hawley, B. Craigo *et al.*, Room-temperature ferroelectricity in strained SrTiO₃, *Nature (London)* **430**, 758 (2004).
- [36] W. Zhong and D. Vanderbilt, Competing structural instabilities in cubic perovskites, *Phys. Rev. Lett.* **74**, 2587 (1995).
- [37] W. Zhong and D. Vanderbilt, Effect of quantum fluctuations on structural phase transitions in SrTiO₃ and BaTiO₃, *Phys. Rev. B* **53**, 5047 (1996).
- [38] N. Sai and D. Vanderbilt, First-principles study of ferroelectric and antiferrodistortive instabilities in tetragonal SrTiO₃, *Phys. Rev. B* **62**, 13942 (2000).
- [39] J. C. Slater, The Lorentz correction in barium titanate, *Phys. Rev.* **78**, 748 (1950).
- [40] J. H. Barrett, Dielectric constant in perovskite type crystals, *Phys. Rev.* **86**, 118 (1952).
- [41] H. Fujishita, S. Kitazawa, M. Saito, R. Ishisaka, H. Okamoto, and T. Yamaguchi, Quantum paraelectric states in SrTiO₃ and KTaO₃: Barrett model, Vendik model, and quantum criticality, *J. Phys. Soc. Jpn.* **85**, 074703 (2016).
- [42] E. Salje, B. Wruck, and H. Thomas, Order-parameter saturation and low-temperature extension of Landau theory, *Z. Phys. B: Condens. Matter* **82**, 399 (1991).

- [43] E. Salje, B. Wruck, and S. Marais, Order parameter saturation at low temperatures—Numerical results for displacive and O/D systems, *Ferroelectrics* **124**, 185 (1991).
- [44] S. A. Hayward and E. K. H. Salje, Cubic-tetragonal phase transition in SrTiO₃ revisited: Landau theory and transition mechanism, *Phase Transit.* **68**, 501 (1999).
- [45] D. M. Ceperley, Path integrals in the theory of condensed helium, *Rev. Mod. Phys.* **67**, 279 (1995).
- [46] L. Ranalli, C. Verdi, L. Monacelli, G. Kresse, M. Calandra, and C. Franchini, Temperature-dependent anharmonic phonons in quantum paraelectric KTaO₃ by first principles and machine-learned force fields, *Adv. Quantum Technol.* **6**, 2200131 (2023).
- [47] C. Verdi, L. Ranalli, C. Franchini, and G. Kresse, Quantum paraelectricity and structural phase transitions in strontium titanate beyond density functional theory, *Phys. Rev. Mater.* **7**, L030801 (2023).
- [48] R. Cabassi, S. Checchia, G. Trevisi, and M. Scavini, Low temperature ferroelectricity in strontium titanate domain walls detected by depolarization pyrocurrents, *Mater. Today Commun.* **28**, 102742 (2021).
- [49] W. Zhong, R. D. King-Smith, and D. Vanderbilt, Giant LO-TO splittings in perovskite ferroelectrics, *Phys. Rev. Lett.* **72**, 3618 (1994).
- [50] P. Ghosez, X. Gonze, P. Lambin, and J.-P. Michenaud, Born effective charges of barium titanate: Band-by-band decomposition and sensitivity to structural features, *Phys. Rev. B* **51**, 6765 (1995).
- [51] P. Ghosez, J.-P. Michenaud, and X. Gonze, Dynamical atomic charges: The case of ABO₃ compounds, *Phys. Rev. B* **58**, 6224 (1998).
- [52] M. Ceriotti, J. More, and D. E. Manolopoulos, I-PI: A Python interface for *ab initio* path integral molecular dynamics simulations, *Comput. Phys. Commun.* **185**, 1019 (2014).
- [53] I. Errea, M. Calandra, and F. Mauri, First-principles theory of anharmonicity and the inverse isotope effect in superconducting palladium-hydride compounds, *Phys. Rev. Lett.* **111**, 177002 (2013).
- [54] L. Monacelli, R. Bianco, M. Cherubini, M. Calandra, I. Errea, and F. Mauri, The stochastic self-consistent harmonic approximation: Calculating vibrational properties of materials with full quantum and anharmonic effects, *J. Phys.: Condens. Matter* **33**, 363001 (2021).
- [55] T. Atanackovic and A. Guran, *Theory of Elasticity for Scientists and Engineers* (Birkhäuser, Boston, 2000).
- [56] N. Provatas and K. Elder, *Phase-Field Methods in Materials Science and Engineering*, 1st ed. (Wiley-VCH, Weinheim, Germany, 2010).
- [57] A. Khachaturyan, *Theory of Structural Transformations in Solids* (John Wiley & Sons, Inc., New York, 1983).
- [58] A. G. Khachaturyan, S. Semenovskaya, and T. Tsakalakos, Elastic strain energy of inhomogeneous solids, *Phys. Rev. B* **52**, 15909 (1995).
- [59] H.-L. Hu and L.-Q. Chen, Three-dimensional computer simulation of ferroelectric domain formation, *J. Am. Ceram. Soc.* **81**, 492 (1998).
- [60] J. Hlinka and E. Klotins, Application of elastostatic Green function tensor technique to electrostriction in cubic, hexagonal and orthorhombic crystals, *J. Phys.: Condens. Matter* **15**, 5755 (2003).
- [61] P. Marton and J. Hlinka, Simulation of domain patterns in BaTiO₃, *Phase Transit.* **79**, 467 (2006).
- [62] N. A. Pertsev, A. G. Zembilgotov, and A. K. Tagantsev, Effect of mechanical boundary conditions on phase diagrams of epitaxial ferroelectric thin films, *Phys. Rev. Lett.* **80**, 1988 (1998).
- [63] K. M. Rabe, Theoretical investigations of epitaxial strain effects in ferroelectric oxide thin films and superlattices, *Curr. Opin. Solid State Mater. Sci.* **9**, 122 (2005).
- [64] R. Feinman, Pytorch-minimize: A library for numerical optimization with Autograd, <https://github.com/rfeinman/pytorch-minimize> (2021).
- [65] J. Nocedal and S. J. Wright, Trust-region methods, *Numerical Optimization* (Springer, New York, 2006), pp. 68–69, 171.